Flash microwave synthesis of trevorite nanoparticles

C. Bousquet-Berthelin*, D. Chaumont, D. Stuerga

*NANOSCIENCES-GERM (Groupe d'Etudes et de Recherches en Microondes), I.C.B. (Institut Carnot de Bourgogne), UMR 5209 CNRS,
Université de Bourgogne, 9 Avenue Alain Savary, B.P. 47870, 21078 Dijon Cedex, France*

Abstract

Nickel ferrite nanoparticles have several possible applications as cathode materials for rechargeable batteries, named "lithium-ion" batteries. In this study, $NiFe_2O_4$ was prepared by microwave induced thermohydrolysis. The obtained nanoparticles were characterized by scanning electron microscopy (SEM) and energy dispersive X-ray spectroscopy (EDX), X-ray diffraction (XRD), BET method, transmission electron microscopy (TEM) and small angle X-ray scattering (SAXS). All the results show that the microwave one-step flash synthesis leads in a very short time to $NiFe_2O_4$ nanoparticles with elementary particles size close to 4–5 nm, and high specific surfaces (close to $240\,m^2/g$). Thus, microwave heating appears as an efficient source of energy to produce quickly nanoparticles with complex composition as ferrite.
© 2008 Elsevier Inc. All rights reserved.

Keywords: $NiFe_2O_4$; Microwave heating; Synthesis; Hydrothermal; Nanoparticles; Nanomaterial; SAXS

1. Introduction

In 1990, Sony [1] surprised the "battery world" by abandoning rechargeable lithium-metal battery development to introduce a new concept, which they named "Li ion". The lithium-metal anode was replaced by a lithium-storage material while the cathode is a lithium-containing compound [2–5]. Compounds with spinel structure are investigated as possible host materials for the insertion of small electron-donor atoms [6–8]. These solids present a framework lattice that provides a three-dimensional interstitial space for accommodating the inserted elements.

The unit formula of spinel compound is commonly written as AB_2X_4. The space group is $Fd\bar{3}m$. The unit cell consists in a cubic close-packed array of X anions with one-eighth of the tetrahedral sites (Td, 87% unoccupied) and one-half of the octahedral ones (Oh, 50% unoccupied) filled by cations. In a *normal spinel*, the A cations are placed on Td sites, and B cations on the Oh ones. In the *inverse spinel*, the A cations are now randomly placed on the Oh sites, half of B cations are on the Td sites and the rest of B cations are on the Oh sites [9]. Then, spinel structures exhibit a high proportion of unoccupied crystallographic sites available for lithium ions. Moreover, it is crucial that the insertion process do not modify the structure of host material. Some experimental results show that spinel materials seem interesting candidates as electrodes in lithium-ion batteries due to their reversible lithium insertion properties [10,11].

The nickel ferrite oxide $NiFe_2O_4$ named trevorite has been chosen because of its numerous applications in battery electrodes, but also for others properties as anti-corrosion protection or magnetic characteristics [12]. It is an inverse spinel structure with O atoms on ($32e$) positions, Ni^{2+} ions on ($16d$) octahedral sites, and Fe^{3+} ions distributed on ($8a$) tetrahedral sites and ($16d$) octahedral sites [13], as shown in the following formula:

$$(Fe_1^{3+})_{8a}[Ni_1^{2+}Fe_1^{3+}]_{16d}O_{4\ 32e}^{2-}.$$
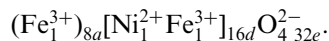
Furthermore, much attention has recently been devoted to the controlled preparation of nanometer-size materials because of their potential applications in high microelectronic devices [14,15], ceramic research and medicine [16,17]. Thus, the development of new materials leads to new methods for their preparation. Conventional synthesis

---

*Corresponding author. Fax: +33 3 80 39 61 32.

E-mail address: christelle.bousquet@u-bourgogne.fr
(C. Bousquet-Berthelin).

methods as solid-state reaction, sintering reaction, decomposition of carbonates or nitrates and coprecipitation, required high temperature and very long processing to obtain oxides particles.

Microwave heating is an emerging technology that uses the ability of liquids and solids to transform electromagnetic energy into heat. Since the mid-90s, more than 90 papers dealing with inorganic compounds synthesis have been published. Among these works, NiFe$_2$O$_4$ ferrite has been firstly produced by microwave route [18,19]. More informations about microwave–material interactions, dielectric properties, key ingredients for mastery of chemical microwave process and laboratory or pilot-scale reactors should be found in Refs. [20] and [21], respectively.

Specific properties of microwave heating are core heating and high energy density close to several kW/cm^3. Microwave treatment of solutions has been carried out by means of an original device designed by the authors, the RAMO system (French acronym of Réacteur Auto-clave MicroOnde [21]). This experimental device is constituted by a microwave applicator associated with an autoclave. The microwave oven and the reactor are specially designed by the authors. Compared to domestic ovens or laboratory digesters (CEM, Millestone), our device allows higher electric field strengths for heated sample. The induced core heating allows faster heating of reactants and higher temperature than conductive heating systems. The plunger control the resonant frequency of the cavity and the effective cavity power would be increase by three orders of magnitude. Heating rates close to several degrees per second can be reached with this laboratory device [22]. Our device allowed preparation of several kinds of nanomaterials as iron oxides [23], zirconia [24,25] titanium oxide [26], nanocomposites [27,28] and manganese oxide [29].

This work presents the first attempt to adapt and improve the microwave one-step flash synthesis for the production of NiFe$_2$O$_4$ ferrite. Conventional operating conditions are generally based on salts aqueous solutions using precipitation of hydroxide in KOH. The aim of this work is to adapt and improve our microwave operating conditions using alcoholic solution with sodium ethoxide (EtONa) as a base. Obviously, the products will be compared with those prepared with the others microwave conditions [18,19,30,31].

Operating conditions: Our simplest method for the generation of uniform colloidal metal oxides is based on microwave thermohydrolysis of metal salt solutions [23–29]. It is well known that most polyvalent cations readily hydrolyze, and that deprotonation of coordinated water molecules is greatly accelerated with increasing temperature. Since hydrolysis products are intermediates to precipitation of metal oxides, these species can be generated at the proper rate to eventually yield nanoparticles by the adjustment of heating rate, temperature and

pH. The mechanism of hydroxylation or olation reaction involves a scheme given by Eq. (1),

$$[M(OH_2)_N]^{z+} + hH_2O \rightarrow [M(OH)_h(OH_2)_{N-h}]^{(z-h)+} + hH_3O^+ \tag{1}$$
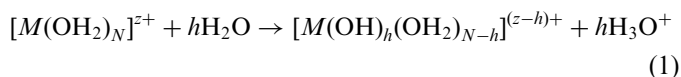
whereas the oxolation reaction involves a scheme given by Eq. (2),

$$n[M(OH)_h(OH_2)_{N-h}]^{(z-h)+} + qH_2O$$
$$\rightarrow [M_n(OH)_{nh+q}(OH_2)_{n(N-h)-q}]^{(nz-nh-q)+} + qH_3O^+. \tag{2}$$
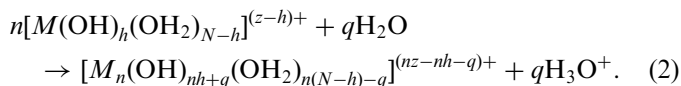
Obviously, theses complexes act as precursors to nucleation and they affect the particle growth. The composition and the rate of generation of these solutes, controlled by heating rate, will determine the chemical and physical natures of the resulting precipitate.

However, microwave thermohydrolysis of nickel salts is impossible. The authors have defined operating conditions able to facilitate concomitant olation and oxolation reactions for iron and nickel precursors. They used ethanol and sodium ethoxide as associated base. The general balance of the reactional scheme is given by Eq. (3),

$$NiCl_2 + 3FeCl_3 + 8NaOEt + 4H_2O \rightarrow NiFe_2O_4$$
$$+ 8NaCl + 8EtOH. \tag{3}$$
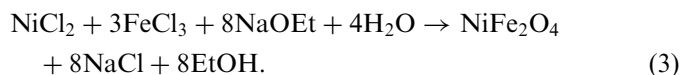
According to this reaction scheme, side product is sodium chloride. This side product elimination will involve several aqueous washing steps.

2. Experimental section

2.1. Preparation

Nickel(II) chloride (NiCl$_2 \cdot 6H_2O$), iron(III) chloride (FeCl$_3 \cdot 6H_2O$) and a base (sodium ethoxide, EtONa) were dissolved into ethanol in order to obtain 0.15, 0.30 and 1.2 M solutions, respectively. The reactants were thus placed in equal volumes in a teflon flask inserted within a polyetherimide flask. The final solution (with a volume close to 20 cm^3) was submitted to a microwave irradiation with the help of an autoclave microwave heating device named RAMO presented in Fig. 1 [21], and designed by the authors. The microwave generator was operated at 2.45 GHz. Solutions were heated under argon atmosphere to avoid sparking risk with flammable solvents. A fiber-optic thermometry system, a pressure transducer and a manometer allow to measure simultaneously the temperature and the pressure within the reactor. The system is controlled by pressure because this parameter reaches steady state more quickly than temperature, and the microwave power is adjusted to keep a constant pressure within the vessel. This experimental device is able to raise the temperature from ambient to 200 °C in less than 20 s according to the microwave power selected (between 1 and 2 kW). In our operating conditions, the microwave power was equal to 1 kW, the pressure reached 11 bar corresponding to a temperature close to 160 °C, and the irradiation
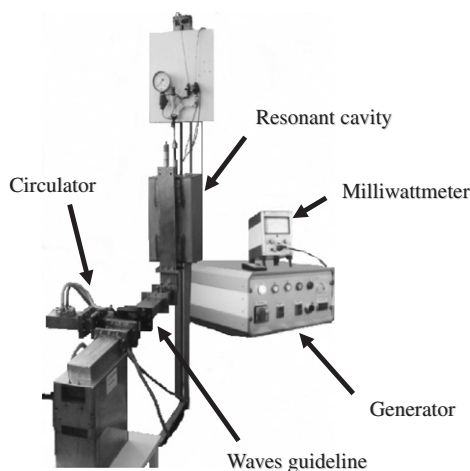
Fig. 1. Presentation of microwave autoclave reactor RAMO.

time was 5 min. After the treatment, the samples were cooled at room temperature, then washed about 10 times with distilled water and with alcohol after. After drying at room temperature, a brownish powder was obtained. A test with a magnet revealed that the powder obtained was magnetic, as confirmed in literature [12].

2.2. Characterization

X-ray powder diffraction (XRD) pattern was firstly used and recorded on a Siemens D-5000 diffractometer using $CuK\alpha$ radiation ($\lambda = 1.5406$ Å). Fixed graphite monochromator guarantee an optimum signal/background ratio with maximum stability. A calculation with the Scherrer formula allowed to reach the particles size.

A scanning electron microscope (SEM) equipped with energy dispersive X-ray spectroscopy (EDX) was firstly used to characterize the synthesized material. The SEM is a Jeol 6400 S device working at 20 keV; the energy dispersive spectrometer is an OXFORD INSTRUMENTS—INCA ENERGY apparatus recording quantum energies between 1 and 10 keV. The characteristic X-ray spectra provide qualitative elemental composition of the studied sample. The $NiFe_2O_4$ powder was dispersed on self-adhesive carbon-coated grids. As the trevorite was isolant, a thin film of carbon was deposited above.

The BET (Brunauer–Emmett–Teller) method was used to calculate the specific area of oxide particles. It consists of studying a gas absorption or desorption (nitrogen in our case) by the considered material with an AUTOSORB1 device.

The morphology of the particles was examined by transmission electron microscopy (TEM) in a HITACHI H600 model. The particles were dispersed into ethanol. After ultrasonic treatment, the suspension was deposited on carbon-coated grids and further evaporated.

Finally, small angle X-ray scattering (SAXS) analysis was used to investigate the structure and the size of produced particles. The SAXS analysis was performed at the Laboratorio Nacional de Luz Sincroton (LNLS) at Campinas (Brazil). A $\lambda = 1.608$ Å wavelength was used. The samples were placed on a 1 mm thick cell with parallel thin Kapton windows. The X-ray beam went through the sample and the scattering intensity, after the cell, was recorded on a linear detector ($I(q)$ vs. q where q was the scattering vector $q = 2\pi \sin\theta/\lambda$ and θ, the scattering angle measured from the direct beam). The sample to detector distance was 666.9 mm. The parasitic scattering produced by collimating slits, Kapton windows, and air was substracted from the total measured scattering intensity.

3. Results and discussion

3.1. Structural analysis

The results of microwave heating experiments showed that the dissolution of the precursors $NiCl_2 \cdot 6H_2O$, $FeCl_3 \cdot 6H_2O$ and base (sodium ethoxide, EtONa) into ethanol could absorb microwave radiation efficiently.

X-ray diffraction was first lead on raw material. XRD lines are very broadened due to nanometric size of particles. Hence, XRD indexation and phase identification are both very difficult. Consequently, powder annealing at 850 °C during 1 h was also realized. Figs. 2 and 3a describe XRD patterns obtained before and after thermal treatment, respectively; typical XRD pattern of $NiFe_2O_4$ is obtained in Fig. 3a. All the diffraction lines can be indexed on a face-centered cubic unit cell, except a peak at 33° (2θ scale). This one is assigned to the principal peak ($I = 100$) of NaCl phase. In fact, the reactional mechanism showed that NaCl occurs during the reaction (see Eq. (3)). Consequently, we can suppose that the protocole initially expressed by the authors and applied here for $NiFe_2O_4$ does not plan enough washings, if we take into account the important quantity of generated NaCl during reaction. Thus, recrystallized material was washing again several times, and studied by XRD. The obtained diffractogramm (Fig. 3b) shows a typical pattern of spinel structure, exempt of NaCl traces. The parameter cell could be thus easily calculated, with (311) and (400) lines. Applying Eqs. (4)
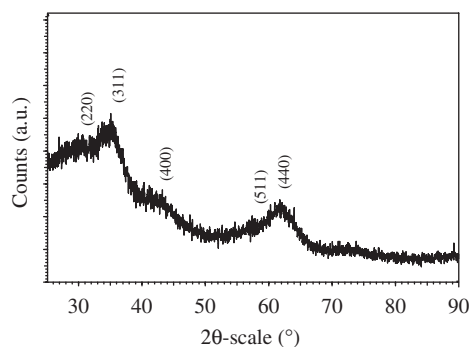

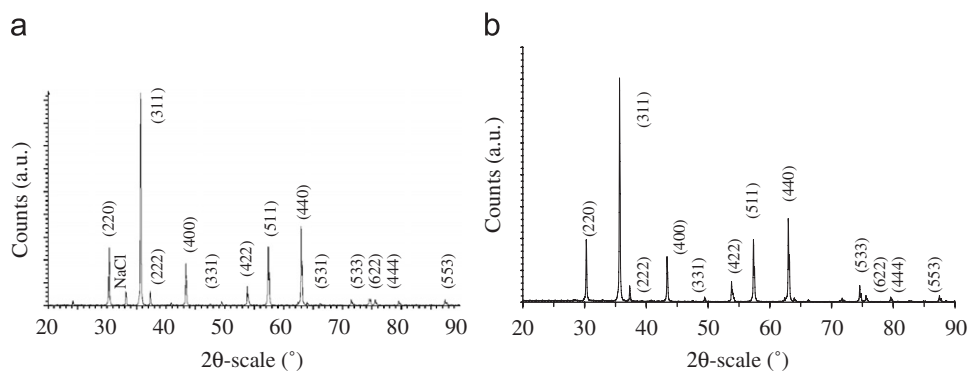Fig. 2. XRD pattern (using $CuK\alpha$) of $NiFe_2O_4$ synthetized by microwave heating.

Fig. 3. XRD pattern (using CuKα) of NiFe$_2$O$_4$ after calcination: (a) initial crystallized material; (b) crystallized material after additional washings.

Table 1
Cell parameters of NiFe$_2$O$_4$

	a (Å)	
	In Fig. 2	In Fig. 3b
(311) line	8.8 (with $2\theta = 33°$) 8.1 (with $2\theta = 37°$)	8.335
(400) line	8.6 (with $2\theta = 61°$) 8.1 (with $2\theta = 63°$)	8.340
Averaged a (Å)	8.4 ± 0.4	8.337

and (5), the calculated averaged value was $a = 8.337$ Å, which is in good agreement with the JCPDS card number 10-325 ($a = 8.339$ Å). In a second time, we tried to evaluate in the same way the cell parameter using Fig. 2 pattern, taking into account peak broadening. It is an approximate calculation and not a precise one, considering that we can be sure that the desired material has been obtained (see Fig. 3). So, a parameter range was calculated and found close to 8.4 ± 0.4 Å. Table 1 summarizes found values of cell parameter.

$$2d \sin \theta = \lambda_{CuK\alpha} \quad (4)$$

and

$$d_{cubic} = \frac{a}{\sqrt{(h^2 + k^2 + l^2)}}. \quad (5)$$

We can consider that our results are in good agreement with the theory if we take into account the difficulty to calculate precisely this value with the broadened diffraction lines. In fact, these peaks are expanded and not well defined because of the probable nanometric size of the trevorite particles. In order to confirm this hypothesis, the Scherrer formula [32] was applied to find the diameter of the particles. After calculation from several peaks of Fig. 2, the found coherent field size was close to 4–5 nm. Moreover, the same value of crystallite size was obtained in all directions (i.e. for several reticular

planes), indicating a spherical form of the particles. Moreover, thermal treatment (Fig. 3) induced recrystallization and so growth of nanoparticles with average size close to 137 nm.

Moreover, the same reactants have been heated with conventional heating modes as electric hotplate in order to compare with microwave treatment. The heating time was 1 h at boiling temperature of ethanol (78 °C). Precipitation reaction has not been observed for samples with and without conventional treatment. The authors have to induce precipitation by adding sodium hydroxide to samples with and without conventional thermal treatment. Several washings have been necessary to eliminate side products as sodium chloride and hydroxide. Reaction rate is very slight and the red obtained powder is amorphous according to X-ray powder diffraction. Powder annealing at 850 °C during 1 h was done. In fact, NiFe$_2$O$_4$ is widely minority. XRD experiment shows that sample is constituted of NiO and the whole filiation of iron(I) and iron(II) oxides as δ-FeOOH, Fe$_3$O$_4$, γ-Fe$_2$O$_3$ and finally α-Fe$_2$O$_3$. These compounds are produced during annealing of amorphous powder.

According to these comparative experiments, conventional heating does not allow to synthesize trevorite particles. The boiling temperature under atmospheric pressure of ethanol (78 °C) is not sufficient to induce olation and oxolation reactions. Our microwave operating conditions with temperature close to 160 °C can induce inorganic condensations within initial solution. This fact has been already observed by the authors: they have induced one-step synthesis of α-Fe$_2$O$_3$ without intermediate products as oxyhydroxides (α, β or δ-FeOOH) in opposition to conventional heating conditions where they are frequently observed [23]. In conventional heating conditions, α-Fe$_2$O$_3$ is obtained by solid transformation of FeOOH.

Results of powder EDX analysis are summarized in Table 2. They revealed higher contents of O atoms, and inferior ones of Fe and Ni. Moreover, small amounts or traces of Na and Cl were detected. They are produced from reaction between metal chlorides and sodium ethoxide, leading to sodium chloride and metal ethoxides. Atomic

percentages of main elements are close to theoretical ones (see Table 2). Moreover, after synthesis, an averaged Fe/Ni ratio close 2.1 was found, which is a good agreement with the theory (Fe/Ni = 2). Several results are given in Table 2 in order to evidence homogeneous characteristics of the synthesized powder (the Fe/Ni ratio being constant for each spectrum). Furthermore, the O atoms content was more than the theoretical one because of the classical over-estimation concerning weak elements analysis (pollution, oxidation, etc.). However, we could interpret this Fe/Ni ratio value (2.1) as a deficit of Ni cations or an excess of Fe cations. More clearly, the synthesized trevorite contained certainly Fe^{2+} cations instead of Ni^{2+} ones, with a reduction of Fe^{3+} cations. Thus, the theoretical formula $Ni_1^{2+}Fe_2^{3+}O_4^{2-}$ can be rewritten as following [33]:

$$Ni_{1-x}^{2+}Fe_x^{2+}Fe_2^{3+}O_4^{2-} \quad \text{with } x = 0.03.$$
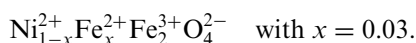
Moreover, an EDX analysis on trevorite particles (the ones obtained after additional washings) was performed and no revealed presence of others elements.

In consequence, it can be concluded that our microwave operating conditions allowed production of well-crystallized nanoparticles of $NiFe_2O_4$.

3.2. Morphological analysis

In order to calculate the specific area of the obtained nanoparticles, the BET method was used [34]. The determinate specific area value was about $234\,m^2/g$ and the particle size was found equal to 4.7 nm, which is very close to the Scherrer formula one.

Trevorite particles were also studied by transmission electron microscopy. The morphology of $NiFe_2O_4$ can be examined in Fig. 4. Pictures showed spherical and monodispersed particles. The measured diameter was about 5 nm as found by DRX and BET method.

SAXS provide an averaged description of the system. Fig. 5 shows for the trevorite sample, the scattering intensity I vs. the scattering vector q, in a double logarithmic plot. This double logarithmic plot evidenced three regions with different slopes. The first part (for $q < 0.079\,\text{Å}^{-1}$) was attributed to particles with a diameter bigger than 16 nm (in first approximation, maximum size is bigger than $2/q_{mini}$). The slope value equal to -2.2 could be interpreted using the fractal theory and indicate that the particles are not dense. These particles have been observed by TEM. In the second part (for $0.079\,\text{Å}^{-1} < q < 0.290\,\text{Å}^{-1}$), the scattering is probably due to scattering

Table 2
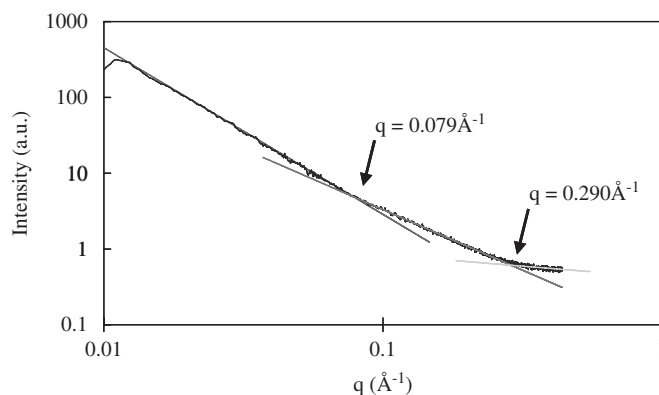Elemental compositions (at%) of $NiFe_2O_4$ material obtained by EDX analysis and theoretical contents

	Element (%)						
	O	Fe	Ni	Na	Cl	Total	Ratio Fe/Ni
Spectrum 1	65.4	23.4	10.7	0.2	0.3	100.0	2.2
Spectrum 2	57.8	28.5	13.3	0	0.4	100.0	2.1
Spectrum 3	66.0	22.2	11.6	0	0.2	100.0	1.9
Spectrum 4	61.9	24.6	12.4	0.6	0.5	100.0	2.0
Spectrum 5	68.7	20.4	9.8	0.6	0.5	100.0	2.1
Average	64.0	23.8	11.6	0.3	0.4	100.0	2.1
Theory	57.1	28.6	14.3	0	0	100.0	2.0
Difference (%)	+12.0	−16.8	−18.8	–	–	–	–

Fig. 5. SAXS intensity vs. q (scattering vector) in double logarithmic plot for $NiFe_2O_4$.
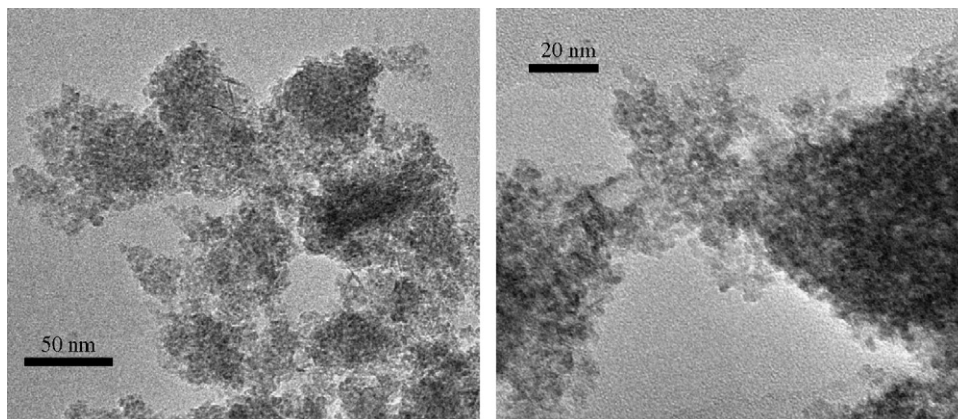

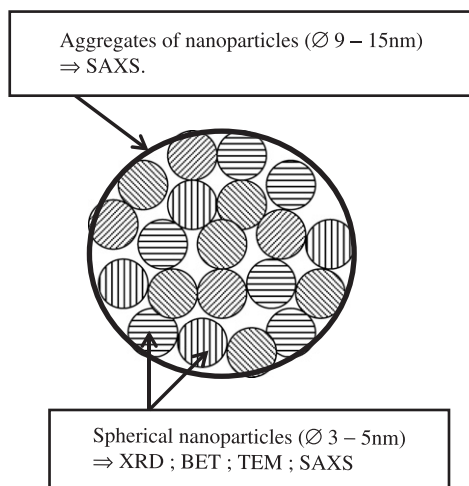Fig. 4. TEM patterns of $NiFe_2O_4$ with different enlarging.

Fig. 6. Aggregation scheme.

elements (pores or particles) with mean size around $2\,nm$ (deduced from the cross-point q, size $\approx 2/q_{\text{croos-point}}$) but with a large polydispersity. They were initially identified by BET method and the XRD experiments showed monocrystalline particles with a diameter close to 4–5 nm. Finally, the scattering intensity in the last region (for $q > 0.290\,\text{Å}^{-1}$) could be attributed to high electronic densities of the trevorite cell.

The scheme described by Fig. 6 summarizes the results obtained with the different characterization techniques.

4. Conclusions

In conclusion, microwave heating of alcoholic solutions of nickel and iron salts leads in a very short time (a few minutes) to $NiFe_2O_4$ nanoparticles with elementary particles size close to 4–5 nm. Powders with high specific surfaces are produced at low temperature (160 °C). Grain size and crystallinity could be increased by further thermal annealing. Our operating conditions using ethanol, nickel and iron chloride salts are cheaper and more rustic comparing to classical sol–gel operating conditions using others alkoxides. The RAMO system associates advantages solution nucleation processes with microwave heating (core heating and heating rate). Microwave heating appears as an efficient source of energy to produce nanoparticles with complex composition as ferrite.

The main difference between similar ferrites produced using aqueous solutions and microwave oven [19,30] is a consequent time saving (several minutes). Moreover, averaged size is slightly small. The authors have shown that sodium ethoxide used instead of potassium hydroxide enhance crystallization and surface area [24–27]. Due to value of surface area, our powder could have catalytic properties enhanced compared to conventional powder; this point should be tested in the future. Despite nanocrystals, powders are systematically composed of several aggregation levels overlapped and typical size of lumps is close to micrometer (Fig. 6). Further work is required to give a better understanding of this agglomeration process.

References

[1] T. Nagaura, K. Tozawa, Prog. Batt. Sol. Cells 9 (1990) 209.
[2] C. Vincent, IEE Rev. 45 (2) (1999) 65.
[3] M. Broussely, P. Biensan, B. Simon, Electrochem. Acta 45 (1999) 3.
[4] G. Maurin, C. Bousquet, F. Henn, P. Bernier, R. Almairac, B. Simon, Chem. Phys. Lett. 312 (1) (1999) 14.
[5] H. Chen, X. Qiu, W. Zhu, P. Hagenmuller, Electrochem. Commun. 4 (2002) 488.
[6] M. Eisenberg, J. Electrochem. Soc. 127 (1980) 2382.
[7] A.C.W.P. James, B. Ellis, J.B. Goodenough, Solid State Ionics 27 (1988) 45.
[8] M. Pernet, P. Strobel, B. Bonnet, P. Bordet, Solid State Ionics 66 (1993) 259.
[9] A.F. Wells, Structural Inorganic Chemistry, fourth ed., Clarendon Press, Oxford, 1975.
[10] C. Bousquet, C. Pérez-Vicente, A. Krämer, J.L. Tirado, J. Olivier-Fourcade, J.C. Jumas, J. Mater. Chem. 8 (6) (1998) 1399.
[11] C. Bousquet, A. Krämer, C. Pérez-Vicente, J.L. Tirado, J. Olivier-Fourcade, J.C. Jumas, J. Solid State Chem. 134 (1997) 238.
[12] J. Liu, H. He, X. Jin, Z. Hao, Z. Hu, Mater. Res. Bull. 36 (2001) 2357.
[13] A.S. Albuquerque, J.D. Ardisson, W.A.A. Macedo, J.L. López, R. Paniago, A.I.C. Persiano, J. Magn. Magn. Mater. 226–230 (2001) 1379.
[14] F. Mazaleyrat, L.K. varga, J. Magn. Magn. Mater. 215/216 (2000) 253.
[15] J. Petzold, J. Magn. Magn. Mater. 242–245 (Pt. I) (2002) 84.
[16] M.A. Riley, A.D. Walmsley, J.D. Speight, I.R. Harris, Mater. Sci. Technol. 18 (2002) 1.
[17] C.R. Martin, D.T. Mitchell, Anal. Chem. (1998) 322A.
[18] S. Komarneni, M.C. D'Arrigo, C. Leonelli, G.C. Pellacani, H. Katsuki, J. Am. Ceram. Soc. 81 (11) (1998) 3041.
[19] J.H. Lee, C.K. Kim, S. Katoh, R. Murakami, J. Alloys Compd. 325 (1/2) (2001) 276.
[20] D. Stuerga, in: A. Loupy (Ed.), Chapter 1, Microwave–Material Interactions and Dielectric Properties, Key Ingredients for Mastery of Chemical Processes in Microwaves in Organic Synthesis, second ed. completely revised and enlarged edition, Wiley-VCH, Weinheim, Germany, 2006.
[21] B. Ondruschka, W. Bonrath, D. Stuerga, in: A. Loupy (Ed.), Chapter 2, Development and Design of Laboratory and Pilot Scale Reactors for Microwave-assisted Chemistry in Microwaves in Organic Synthesis, second ed. completely revised and enlarged edition, Wiley-VCH, Weinheim, Germany, 2006.
[22] D. Stuerga, P. Gaillard, Tetrahedron 52 (15) (1996) 5505.
[23] K. Bellon, P. Rigneau I. Zahreddine, D. Stuerga, Eur. Phys. J. Appl. Phys. AP 7 (1999) 41.
[24] K. Bellon, D. Chaumont, D. Stuerga, J. Mater. Res. 16 (2001) 9.
[25] L. Combemale, G. Caboche, D. Stuerga, D. Chaumont, Mater. Res. Bull. 40 (2005) 529.
[26] E. Gressel-Michel, D. Chaumont, D. Stuerga, J. Colloid Interface Sci. 285 (2005) 674.

[27] T. Caillot, D. Aymes, D. Stuerga, N. Viart, G. Pourroy, J. Mater. Sci. 37 (2002) 5153.

[28] T. Caillot, G. Pourroy, D. Stuerga, J. Solid State Chem. 177 (2004) 3843.

[29] C. Bousquet-Berthelin, D. Stuerga, J. Mater. Sci. Lett. 40 (2005) 253.

[30] G. Wang, G. Whittaker, A. Harrison, L. Song, Mater. Res. Bull. 33 (11) (1998) 1571.

[31] C.K. Kim, J.H. Lee, S. Katoh, R. Murakami, M. Yoshimura, Mater. Res. Bull. 36 (12) (2001) 2241.

[32] A.L. Patterson, Phys. Rev. 56 (1939) 978.

[33] E. Barrado, F. Prieto, F.J. Garay, J. Medina, M. Vega, Electrochim. Acta 47 (2002) 1959.

[34] S. Brunauer, P.H. Emmett, E. Teller, J. Am. Chem. Soc. 60 (2) (1938) 309.